Negative-Magnetoresistance Effects in Ti_2O_3†

J. M. HONIG,*§ L. L. VAN ZANDT,‖ T. B. REED, AND J. SOHN‡
Lincoln Laboratory, Massachusetts Institute of Technology, Lexington, Massachusetts 02173
(Received 6 February 1969)

Negative-magnetoresistance phenomena are reported at 4.2°K for single-crystal Ti_2O_3 doped with vanadium in the 0.3–4 at.% range. The results were analyzed by time-dependent perturbation theory in terms of an inelastic scattering mechanism involving magnetic impurities such as Fe^{3+} present at the 10–100 at. ppm level. The vanadium ions are believed to be magnetically inert. It is concluded that the material under study is not antiferromagnetic at 4.2°K.

I. INTRODUCTION

THIS paper is one in a series[1] on electrical properties of titanium sesquioxide; we report here on resistivity, Hall, and magnetoresistance measurements of Ti_2O_3 doped with 0.1 to 4 at.% V_2O_3. The appropriate theory for the interpretation of the negative magnetoresistance effects encountered in the experiments is also developed.

The measurements are deemed to be of interest: first, because they complement earlier investigations on highly purified Ti_2O_3; second, because the negative magnetoresistance effects appear to have been one of the first of their kind reported for any oxide; third, because a quantitative fit of the data with theory sheds further light on the band structure and magnetic properties of Ti_2O_3, concerning which there has been disagreement[2] in the past.

II. EXPERIMENTAL

Large single-crystal boules of Ti_2O_3 doped with controlled amounts of V_2O_3, Cr_2O_3, or Sc_2O_3 were grown from the melt in a resistance-heated furnace by the Czochralsky-Kyropoulos technique as described in an earlier publication.[1] The pure material showed very little evidence of mosaic structure or other disorder.[3]

The total impurity content of samples was analyzed with a mass spectrometer. Vacuum-fusion analyses were also carried out to determine sample contamination by N or C. The impurity content of various samples is shown in Table I.

The single-crystal boules were oriented, and 1×2×8-mm slices were cut along certain crystallographic directions. Electrical leads were attached with In solder, and the crystal was mounted on holders that could be immersed in appropriate cryogenic liquids. Standard magnetoresistance and magneto-Hall experiments were carried out at the Francis Bitter National Magnet Laboratory in fields up to 220 kG.

III. EXPERIMENTAL RESULTS

A. Resistivity and Hall Effect as a Function of Temperature

Resistivities ρ measured at 4.2, 77, and 273°K for a variety of samples in distinct orientations, and doped to varying degrees with different impurities, are listed in Table I. For comparison, we have included the results for a highly purified specimen of Ti_2O_3 (sample 128). Where available, we have also listed the Hall coefficients R measured at 150 kG; these appear to approach the high-field limiting values for R before the onset of quantum effects (Sec. III B).

It is seen that in an undoped and reasonably pure specimen of Ti_2O_3 the resistivity at 4.2°K is considerably in excess of $10^4\,\Omega$ cm and that ρ depends on sample orientation; furthermore, ρ diminishes nearly exponentially with increasing temperatures[1] up to 300°K. By contrast, samples doped nominally with more than 0.5 at.% V exhibit resistivities below $10^{-2}\,\Omega$ cm at 4.2°K which vary only slightly with temperature; the dependence of ρ on sample orientation is small. The high-field Hall coefficients of the doped specimens are very nearly independent of temperature and of crystal orientation. Samples doped with 0.1–0.3 at.% Sc or V exhibit intermediate properties.

B. Magnetoresistance and Magneto-Hall Data

Measurements on the transverse magnetoresistance and magneto-Hall effect were carried out on a majority of the samples listed in Table I. The results at 4.2°K may be summarized as follows: In pure Ti_2O_3, such as sample 128, the magnetoresistance $\Delta\rho/\rho_0$ increases quadratically with the applied field H beyond 220 kG.[1] As successively more dopant is added, $\Delta\rho/\rho_0$ increases less sharply with H; when the doping level approaches 1 at.%, negative-magnetoresistance effects are encountered. These do not depend markedly on doping levels in the range between 1 and 4 at.%.

A typical set of negative-magnetoresistance curves

† This work was sponsored by the U. S. Air Force.
* Present address: Purdue University, West Lafayette, Ind. 47907.
§ Guest Scientist, Francis Bitter National Magnet Laboratory, Cambridge, Mass.
‖ Supported in part by ARPA Institutional Grant No. SD 102 at Purdue University.
‡ Present address: Sperry Rand Corporation, Sudbury, Mass.
[1] J. M. Honig and T. B. Reed, Phys. Rev. **174**, 1020 (1968), hereafter referred to as I. T. B. Reed, R. E. Fahey, and J. M. Honig, Mat. Res. Bull. **2**, 561 (1967).
[2] See, e.g., J. M. Honig, Rev. Mod. Phys. **40**, 748 (1968); D. Adler, *ibid.* **40**, 714 (1968).
[3] A. Arrott (private communication).

TABLE I. Listing of electrical and chemical properties of V-doped Ti_2O_3 samples.

Sample designation	Dopants and principal impurities at.% or at. ppm	Current and field orientation	4.2°K ρ_0 (Ω cm)	4.2°K $\Delta\rho/\rho_0$ (150 kG)	4.2°K R 150 kG cm³/C	77°K ρ_0 Ω cm	77°K $\Delta\rho/\rho_0$ 150 kG	77°K R 150 kG cm³/C	273°K ρ_0 Ω cm	273°K $\Delta\rho/\rho_0$ 150 kG	273°K R 150 kG cm/C
128	No dopant	$I\|\|c$	1.8×10^{5}	+1.6		0.31		+1.2	1.2×10^{-2}	-1.3×10^{-3}	$+8.5\times10^{-2}$
	(N 152 ppm,	$\perp c$	1.3×10^{4}	+1.1		0.21		+1.4	1.0×10^{-2}		$+9.1\times10^{-2}$
	Zr 200 ppm,	$\perp a$	5.4×10^{4}	+1.3		0.66	a	+0.45			
	Hf 310 ppm,	45° c	2.7×10^{4}	+1.4		0.35		+1.0			+0.11
	Fe 50 ppm,	45° a	8.0×10^{4}	+1.4		0.82		+1.0			
	Mg 300 ppm)										
3-143-79	0.19% Se	$I\|\|c$	8.7	+1.5[c]	+0.15	6.1×10^{-2}		+0.12	10 $\times10^{-3}$		
	(N 240 ppm)	22.5°	3.2	+1.6	+0.4 to +4	2.4×10^{-2}		+0.15			
		45°	4.6	+1.6	−1.5 to +0.6	2.7×10^{-2}	a	+0.16	3.8×10^{-3}	b	$+3.5\times10^{-2}$
		67.5°	5.4	+1.6	+0.4 to +1.8	3.4×10^{-2}		+0.19	5.1×10^{-3}		
		$\perp c$	6.5	+1.6	+0.2 to +2.7	3.3×10^{-2}		+0.17	4.4×10^{-3}		$+4.2\times10^{-2}$
3-145-79	0.26% V	$I\|\|c$	1.3	+0.70	+0.04 to +0.40						
	(N 190 ppm	$\perp c$	0.92	+0.62	+0.19						
	Fe 10 ppm)	45°	1.7	+0.70	+0.11	3.1×10^{-2}	3.9×10^{-2}				
496	1.3% Cr	$I\perp c$	2.7×10^{-2}	+0.12	$+1\times10^{-2}$ [d]						
139 M	0.9% V	Unoriented	2.5×10^{-3}	−0.096	−0.10	2.3×10^{-3}	-3.6×10^{-3}	$+8.6\times10^{-3}$	2.2×10^{-3}	-2.5×10^{-4}	$+5\times10^{-3}$
	(Mn 22 ppm)										
359	2% V	Unoriented	2.3×10^{-4}	−0.042[c]	+0.12	2.2×10^{-4}		$+5\times10^{-3}$	2.3×10^{-4}		$+4.4\times10^{-3}$
495	3.8% V	$I\perp c$	5.3×10^{-4}	−0.075	$+1\times10^{-2}$	3.7×10^{-4}	-2×10^{-3}	$+6.4\times10^{-3}$			
	(Fe 80 ppm	$H\|\|c$						to 7.7×10^{-3}			
	Mn 10 ppm										
	N 700 ppm)										
358	1% V	Unoriented	9.8×10^{-4}	−0.091[c]	$+5.5\times10^{-3}$	8.9×10^{-4}		$+5.2\times10^{-3}$	7.5×10^{-4}		$+3.9\times10^{-3}$
88-98	2% V	$I\|\|c$	12 $\times10^{-4}$	−0.085	$+5.0\times10^{-3}$	10.2×10^{-4}	-2.5×10^{-3}	6.3×10^{-3}			
		22.5°	10 $\times10^{-4}$	−0.085	$+6.8\times10^{-3}$	4.9×10^{-4}	-4.0×10^{-3}	7.0×10^{-3}			
		45°	8.2×10^{-4}	−0.083	$+6.5\times10^{-3}$	9.8×10^{-4}	-3.0×10^{-3}	6.7×10^{-3}			
		67.5°	10 $\times10^{-4}$	−0.083	$+6.7\times10^{-3}$	2.0×10^{-4}	-3.0×10^{-3}	6.2×10^{-3}			
		$\perp c$	3.5×10^{-4}	−0.090	$+8.5\times10^{-3}$ [(c)]						
133	2.6% V	$I\|\|c$	15 $\times10^{-4}$	−0.103	$+7.3\times10^{-3}$	1.5×10^{-3}	-3.3×10^{-3}	$+7.4\times10^{-3}$	1.8×10^{-4}	-4.0×10^{-4}	$+5.2\times10^{-3}$
	(N 70 ppm	$\perp c$	8.8×10^{-4}	−0.103	$+14.1\times10^{-3}$	8.9×10^{-4}	-3.6×10^{-3}	+10 $\times10^{-3}$			
	Fe 20 ppm	$\perp a$	12 $\times10^{-4}$	−0.102	$+6.9\times10^{-3}$						
	Mn< 10 ppm)										
110-111	2% V	$I\|\|a$	8.3×10^{-4}	−0.140	$+8.0\times10^{-3}$	8.5×10^{-4}		$+4.0\times10^{-3}$	9.7×10^{-4}		$+3.5\times10^{-3}$
	(N 160 ppm	$\|\|c$	9.5×10^{-4}	−0.094	$+4.5\times10^{-3}$	9.9×10^{-4}		$+4.3\times10^{-3}$			
	Fe 18 ppm	$\|\|b$	13 $\times10^{-4}$	−0.125	$+4.0\times10^{-3}$	12 $\times10^{-4}$		$+4.5\times10^{-3}$	14 $\times10^{-4}$		$+3.9\times10^{-3}$
	C 5 ppm)										

[a] Slightly negative. [b] Barely measurable; negative. [c] Estimated by extrapolation. [d] Field-dependent.

for specimens doped with 2–4 at.% V is displayed in Fig. 1. The effect was found to be insensitive to the alignment of the single crystal relative to the directions of the magnetic field and of current flow (these were always maintained mutually at right angles) and to doping level; hence the curves are truly representative of all samples listed in the bottom half of Table I. The negative magnetoresistance is rather larger than that encountered in the liquid-helium-temperature range for heavily doped elemental or III-IV compound semiconductors[4]; even at $H=220$ kG, the anticipated minimum in magnetoresistance has not yet been approached. Moreover, the effect persists into the liquid-nitrogen- and ice-temperature ranges, though it becomes very small at these temperatures. Indeed, these small negative magnetoresistances were encountered in all samples (including those discussed in I) for which electrical properties have been investigated at 77 and 273°K. To the best of our knowledge, this is the first time that a negative-magnetoresistance effect has been observed far above the liquid-helium-temperature region.

In general, the Hall coefficients were found to be nearly independent of H and of T. However, all samples for which the current direction was in the basal plane exhibited a magneto-Hall effect at 4.2°K of the type shown in Fig. 2. The curve asymptotically approaches a value slightly higher than the constant R value encountered at 77.7°K.

According to the model discussed in Sec. VI, the highly doped specimens are metallic in nature, with a density of holes that is determined by the degree of doping. This stands in contrast to pure Ti_2O_3, which appears to be an intrinsic semiconductor at 4.2°K with a band gap of the order of 0.02 eV.[1] One should expect

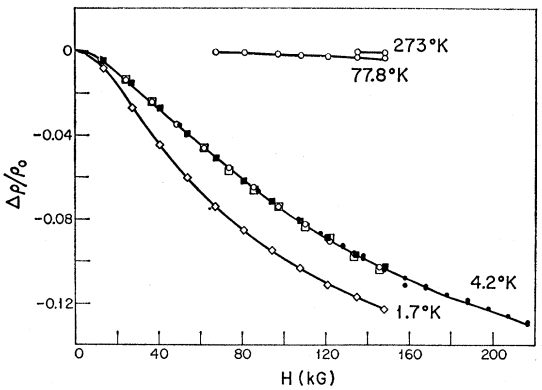

FIG. 1. Negative-magnetoresistance effects in Ti_2O_3 at 1.7, 4.2, 77.8, 273°K. Sample 133, $I \| c$.

[4] See, e.g., H. Fritzsche and K. Lark-Horowitz, Phys. Rev. **99**, 400 (1955); W. Sasaki and Y. Kanai, J. Phys. Soc. Japan **11**, 894 (1956); W. Sasaki, C. Yamanouchi, and G. M. Hatoyama, in *Proceedings of the International Conference on Semiconductor Physics, Prague, 1960* (Academic Press Inc., New York, 1961), p. 159.

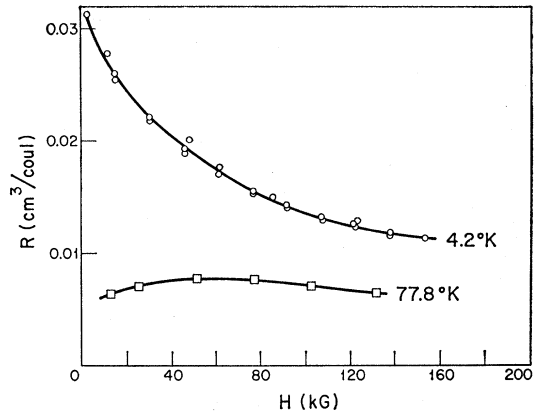

FIG. 2. Magneto-Hall effect in Ti_2O_3 at 4.2 and 77.8°K for sample 4-95, $I \perp c$.

the doped samples to conform to the approximate relation $R=1/n_p ec$. Actually, the observed R values correspond to carrier densities roughly half as large as those computed from the V concentration added to the melt.

IV. THEORY

A. Qualitative Discussion

Our model for the interpretation of our data is a degenerate isotropic electron gas with a well-defined Fermi surface. The electrons interact with randomly located (substitutionally) localized scattering centers which are of two types: magnetic centers possessed of an internal angular degree of freedom with which the carrier spins may interact, and nonmagnetic inert centers. The Ti cations of the host lattice play no role in scattering of carriers. Arguments will later be adduced to show that the V ions are also magnetically inert and represent one set of impurity scattering sites. Magnetic scattering will be linked to the presence of other impurities such as iron for which, in the Fe^{3+} state, there is no spin-orbit coupling. It is these particular centers which are believed to be responsible for the observed negative-magnetoresistance effects.

The magnetic scatterers interact with magnetic fields, whereby different angular momentum states, all degenerate in zero field, are split by the Zeeman energy. Collisions in which the angular momentum state is altered require exchange of energy as well as momentum between colliding hole and scattering center; the amount of energy is proportional to the field. At low temperatures or high fields such collisions become unlikely, either through the lack of unoccupied carrier states at the proper lower energy, or through the lack of excited scatterers to relinquish energy to the carrier. Thus, when energy is transferred to a magnetic scattering center, for example, there are then not enough carriers which meet the energy requirements for placing the center into the next higher quantum level. Increasing the magnetic field thus gradually closes off a

possible relaxation mechanism and thereby decreases the resistivity. By "low temperature" or "high field" we mean to compare the Zeeman energy with the depth of the Fermi zone, kT.

In pure Ti_2O_3, which is an intrinsic semiconductor at 4.2°K, the magnetoresistance is large and positive; this has been interpreted in terms of a standard model in which the scattering is field-independent.[1,2] By doping Ti_2O_3 with 1–4 at.% V_2O_3, sufficient carriers are introduced to render the material degenerate, thereby largely suppressing the positive magnetoresistance. The very conditions necessary for suppression of the positive magnetoresistance, $n_p \gg n_n$, give the degeneracy necessary to obtain a substantial negative magnetoresistance as we have discussed.

The magnetic field responsible for the Zeeman splitting of the magnetic impurity levels involves first the externally applied field, and second, any preexisting molecular field arising from magnetic order; these two contributions must be summed vectorially. An analysis of negative-magnetoresistance effects should thus yield information on the magnitude of the internal magnetic field. As the data show, substantial negative-magnetoresistance effects are encountered even in a small applied field, are nearly independent of sample or magnetic field orientation, and are still increasing in magnitude for applied fields exceeding 200 kG. These facts strongly suggest that the internal magnetic field in Ti_2O_3 is very small, a conclusion that is borne out by the analysis offered below.

In our quantitative analysis we considered the possibility of antiferromagnetic ordering, which was claimed to exist in this material.[5] In this case the internal field would have one orientation on one group of sites and the opposite orientation on another group.[6]

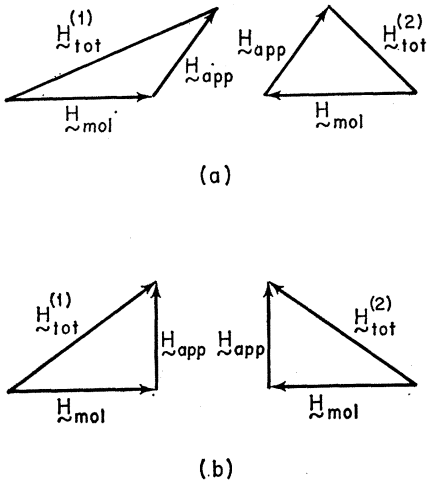

FIG. 3. Two possible relative alignments of the internal, molecular and the external, applied magnetic fields.

Assuming impurity ions to be randomly substituted in cation positions of the host lattice, we should expect two different sets of Zeeman splittings for the two general relative directions of applied and internal fields, as illustrated in Fig. 3(a). However, for certain orientations of the applied field, perpendicular to the internal fields, both Zeeman splittings should be the same; Fig. 3(b) illustrates this case. Thus, while we consider only one chemical type of magnetic impurity, two different kinds of magnetic sites must generally be taken into account.

It should be noted that when the total impurity concentration is small, any preexisting molecular field at impurity sites will differ very little from that of the normal sites. Hence the determination of the total field at a magnetic impurity site should be reasonably representative of the field for the crystal as a whole. Nevertheless, the division of internal fields into two sets is a simplification of fact, as the magnetic scatterers interact with one another. A mechanism for this interaction is the polarization of the gas of carriers by one spin and the interaction of another spin with this polarization, the well-known Ruderman-Kittel-Kasuya-Yosida interaction. Since the range of this interaction grows for smaller Fermi wave vectors ($\mathbf{k}_F$), and since the number of carriers is reduced in our system compared to a typical metal, we should expect a small $\mathbf{k}_F$, and consequently long-range substantial interactions between magnetic scatterers despite their small concentration.

A careful treatment of interactions would greatly complicate our discussion; however, we may allow approximately for such effects. When a magnetic impurity spin is turned by a colliding electron, it interacts both with the field in its location and with its neighbors. The role of the neighbors is thus to modify the effective magnetic field in spin flips. When the external and intrinsic fields are zero, the impurity spins are randomly arranged, and the effects of the interaction tend to average out to a small value. Below the ordering temperature and when the total fields are large, all the magnetic impurity spins tend to align in characteristic directions and the interaction effects will be larger. It is therefore reasonable to approximate the effect of the interactions by a multiplicative phenomenological factor (corrective g factor) in the effective fields, or in the magnetic moments of the impurities. If the most energetically favorable configuration of the impurities is antialignment, this factor is less than unity, as we find it to be. One should note that the tendency to relative antialignment of magnetic impurities is independent of the existence of antiferromagnetism in the crystal. Indeed, it arises from the interaction of these spins with the electron gas. Because the alignment is temperature-dependent, the effective g factor will be likewise. As we shall discuss, it is also possible, and

[5] S. C. Abrahams, Phys. Rev. **130**, 2230 (1963).

[6] This assumes the period of the magnetic ordering to be commensurable with the lattice period. This same assumption is also required to construct a magnetic-ordering theory of the high-temperature resistivity anomaly.

perhaps preferable, to describe the impurity interaction effects in terms of an effective temperature, as is done in the usual theory of high-temperature magnetic susceptibility.

B. Quantitative Development

We now proceed with a quantitative treatment of these ideas. Since the essential features of the derivation have already been outlined by others,[7,8] we discuss only as much detail of the derivation as is necessary to show the incorporation of the special, novel features of our model.

An approximate wave function for an electron gas is provided by a Slater determinant of N one-electron wave functions of the type

$$\frac{1}{\sqrt{\Omega}}e^{i\mathbf{k}\cdot\mathbf{r}}\begin{pmatrix}1\\0\end{pmatrix} \quad \text{or} \quad \frac{1}{\sqrt{\Omega}}e^{i\mathbf{k}\cdot\mathbf{r}}\begin{pmatrix}0\\1\end{pmatrix}. \tag{1}$$

The impurity wave functions are normalized spherical harmonics appropriate to states of angular momentum $\mathcal{S}$ and projection M_s. The total system wave function is a product of spherical harmonics, one for each impurity, and the electron determinant. The electrons interact with scattering centers according to the perturbation

$$H_1=\sum_{\mathbf{R}}[V_{\mathbf{R}}+J_{\mathbf{R}}\{2s_zS_z+s^+S^-+s^-S^+\}]\delta(\mathbf{r}-\mathbf{R}), \tag{2}$$

where S and s refer to impurity and electron spins, and

$$S^{\pm}\equiv S_x\pm iS_y, \quad s^{\pm}\equiv s_x\pm is_y. \tag{3}$$

R is an index running over all impurity sites; for neutral sites $J_{\mathbf{R}}=0$.

The N electrons are distributed over states $\mathbf{k}_\eta$ ($\eta\equiv+$ or $-$) according to the distribution function $f(\mathbf{k}_\pm)$; the $\pm$ sign refers to the electron spin. This function changes through the action of the applied electric field $\mathcal{E}$ according to

$$\left(\frac{df(\mathbf{k}_\pm)}{dt}\right)_{\text{field}}=\frac{e\mathcal{E}}{\hbar}\cdot\nabla_{\mathbf{k}}f(\mathbf{k}_\pm) \tag{4}$$

and also by the action of scattering according to

$$\left(\frac{df(\mathbf{k}_\pm)}{dt}\right)_{\text{coll}}=\sum_{\mathbf{k}',\eta'}\{W(\mathbf{k}'_{\eta'},\mathbf{k}_\eta)f(\mathbf{k}_\eta)[1-f(\mathbf{k}'_{\eta'})] -W(\mathbf{k}_\eta,\mathbf{k}'_{\eta'})f(\mathbf{k}'_{\eta'})[1-f(\mathbf{k}_\eta)]\}; \tag{5}$$

$W(\mathbf{k}'_{\eta'},\mathbf{k}_\eta)$ is the rate of scattering from the state $\mathbf{k}_\eta$ to the state $\mathbf{k}'_{\eta'}$, given that $\mathbf{k}_\eta$ is occupied and $\mathbf{k}'_{\eta'}$ is not. We calculate $W(\mathbf{k}'_{\eta'},\mathbf{k}_\eta)$ by the "golden rule" of first-order time-dependent perturbation theory: For the set of impurity sites,

$$W(\mathbf{k}'_{\eta'},\mathbf{k}_\eta)=(2\pi/\hbar)|\langle j|H_1|i\rangle|^2\delta(\epsilon_i-\epsilon_j). \tag{6}$$

The i and j refer to states of the entire system of electrons and impurity spins, and ϵ_i, ϵ_j are total energies of the electron gas plus the spins.

Because of the random distribution of impurities through the lattice, we may ignore the interference terms between scatterers on different sites, calculating W as a sum of independent scattering rates w from each impurity site. As we mentioned, there are three different types of impurity with which an electron may interact: neutral impurities and magnetic impurities on two magnetically inequivalent sites. The scattering from all sites proceeds independently, so the total rate $W(\mathbf{k}'_{\eta'},\mathbf{k}_\eta)$ may be found by addition of the rates calculated for each single site:

$$W(\mathbf{k}'_{\eta'},\mathbf{k}_\eta)=\sum_{\mathbf{R}}w_{\mathbf{R}}(\mathbf{k}'_{\eta'},\mathbf{k}_\eta)\equiv N\langle\langle w(\mathbf{k}'_{\eta'},\mathbf{k}_\eta)\rangle\rangle, \tag{7}$$

where N is the total number of impurities of all kinds. We elaborate below on the average defined here.

Three types of terms occur for each magnetic scatterer; its spin may be increased, left unchanged, or decreased by the several operators of the perturbation, Eq. (2). We substitute the perturbation into (6), and integrate to obtain matrix elements of (2) between approximate wave functions referred to earlier. This yields the elements of (6) in the form

$$(V_{\mathbf{R}}+2J_{\mathbf{R}}m_sM_s)\delta(m_s,m_s')\delta(M_s,M_s')/\Omega, \tag{8a}$$

$$J_{\mathbf{R}}\delta(m_s',m_s+1)\delta(M_s',M_s-1)\times[\mathcal{S}(\mathcal{S}+1)-M_s(M_s+1)]^{1/2}/\Omega, \tag{8b}$$

$$J_{\mathbf{R}}\delta(m_s',m_s-1)\delta(M_s',M_s+1)\times[\mathcal{S}(\mathcal{S}+1)-M_s(M_s-1)]^{1/2}/\Omega. \tag{8c}$$

The expressions involving radicals and Kronecker deltas are the familiar matrix elements of the angular momentum operators. M_s, M_s' and m_s, m_s' refer to the spin quantum numbers for the scatterer and carriers, respectively, before (unprimed) and after (primed) the collision. These matrix elements, squared, become the components of $w_{\mathbf{R}}(\mathbf{k}'_{\eta'},\mathbf{k}_\eta)$ in (7).

The distribution function $f(\mathbf{k}_\pm)$ is divided into two parts: An equilibrium part given by the Fermi function f_0, and a deviation f_1 from the equilibrium value.

$$f(\mathbf{k}_\pm)=f_0(\mathbf{k})+f_1(\mathbf{k}_\pm). \tag{9}$$

We insert this relation in (5) and obtain three expressions: one independent of $f_1(\mathbf{k}_\pm)$, another of first order in $f_1(\mathbf{k}_\pm)$ and $f_1(\mathbf{k}_\pm')$, and the third of second order. The first expression describes net scattering for the equilibrium situation and vanishes identically. The third expression we discard as inappropriate to a calculation of conductivity, which is a first-order response function. We are left with terms of the form

[7] T. Kasuya, Progr. Theoret. Phys. (Kyoto) **22**, 227 (1959).
[8] A. R. De Vroomen and M. P. Potters, Physica **27**, 657 (1961).

$f_1(\mathbf{k}_\eta)$ multiplied by integrals of $W(\mathbf{k}'_{\eta'},\mathbf{k}_\eta)$ over $\mathbf{k}'_{\eta'}$, and integrals of $W(\mathbf{k}'_{\eta'},\mathbf{k}_\eta)f_1(\mathbf{k}'_{\eta'})$. Assuming inversion symmetry of the system, the reversal of the electric field reverses the current and makes $f_1(\mathbf{k}_\eta)$ odd under the inversion $\mathbf{k}_\eta \leftrightarrow -\mathbf{k}_\eta$. The integrals of $W(\mathbf{k}'_{\eta'},\mathbf{k}_\eta) \times f_1(\mathbf{k}'_{\eta'})$ therefore vanish. Explicit use has been made here of the highly localized form of H_1 [Eq. (2)]. We obtain

$$\left(\frac{df(\mathbf{k}_\pm)}{dt}\right)_{\text{coll}} = \frac{-\Omega}{8\pi^3}\int \{f_1(\mathbf{k}_\pm)W(\mathbf{k}_\pm',\mathbf{k}_\pm)[1-f_0(\mathbf{k}_\pm')] + f_0(\mathbf{k}_\pm')W(\mathbf{k}_\pm,\mathbf{k}_\pm')f_1(\mathbf{k}_\pm) + f_1(\mathbf{k}_\pm)W(\mathbf{k}_\mp',\mathbf{k}_\pm)[1-f_0(\mathbf{k}_\mp')] + f_0(\mathbf{k}_\mp')W(\mathbf{k}_\pm,\mathbf{k}_\mp')f_1(\mathbf{k}_\pm)\} d^3\mathbf{k}'. \quad (10)$$

The functions $W(\mathbf{k}_\pm',\mathbf{k}_\pm)=W(\mathbf{k}_\pm,\mathbf{k}_\pm')$, $W(\mathbf{k}_\mp',\mathbf{k}_\pm)$, and $W(\mathbf{k}_\pm,\mathbf{k}_\mp')$ are taken from (7) and (8). Furthermore, under steady-state conditions the left-hand side of (10) may be replaced with Eq. (4). We obtain

$$\frac{e\mathcal{E}}{\hbar}\cdot\nabla_{\mathbf{k}} f_0 = \frac{2\pi}{8\pi^3\hbar} f_1(\mathbf{k}_\pm) N \left\{ \int \langle\langle (V_R + M_s J_R)^2 \rangle\rangle \delta(E-E') d^3\mathbf{k}' + \int \langle\langle J_R^2 \zeta^\pm(E,\Delta E)\delta(E'-E\pm\Delta E)\rangle\rangle d^3\mathbf{k}' \right\} \Omega^{-1} \equiv f_1(\mathbf{k}_\pm)/\tau(\mathbf{k}_\pm), \quad (11)$$

where

$$\zeta^\pm \equiv \Lambda^+[1-f_0(E\mp\Delta E)] + \Lambda^- f_0(E\mp\Delta E) \quad (12)$$

and

$$\Lambda^\pm \equiv \mathcal{S}(\mathcal{S}+1) - M_s(M_s \pm 1); \quad (13)$$

ΔE is the Zeeman splitting of the levels and E and E' are the electron energies in the states $\mathbf{k}$ and $\mathbf{k}'$. The $\langle\langle\ \rangle\rangle$ refer to the averaging process necessary to account for the different M_s and distinct types of sites. Let us consider the average in the first term of the curly brackets in (11):

$$N\langle\langle (V_R + M_s J_R)^2 \rangle\rangle \equiv \sum_R (V_R + M_s J_R)^2. \quad (14)$$

The neutral sites contribute a term

$$N_{\text{eff}} V^2 \equiv \sum_l N_l V_l^2 \quad (15)$$

to the sum. Here the left-hand side is an abbreviation for a summation of terms over all species l of neutral sites. The magnetic sites contribute

$$\sum_{R_{\text{mag}}} (V + M_s J)^2. \quad (16)$$

This sum in turn can be decomposed into separate sums over the two different magnetic sites

$$\sum_{R_1} (V + M_s J)^2 + \sum_{R_2} (V + M_s J)^2. \quad (17)$$

Finally, each magnetic impurity is in one of the several states of differing M_s. The probabilities of the several M_s values may be found from the magnitude of the Zeeman splitting appropriate to the site and by use of Boltzmann statistics. Thus we can write

$$\sum_R \langle\langle (V_R + M_s J_R)^2 \rangle\rangle = N_{\text{eff}} V^2 + N_{\text{mag}} \tfrac{1}{2}[\langle (V + M_s J)^2 \rangle_1 + \langle (V + M_s J)^2 \rangle_2], \quad (18)$$

where now the single $\langle\ \rangle_{1,2}$ means a thermodynamic average involving the appropriate local magnetic field. We have used the random distribution of scatters to equate the number of magnetic sites of the two types.

The second term in (11) is treated similarly; there are no contributions from neutral scatterers, and the ΔE in the energy-conservation delta functions must be chosen appropriately for each site. One obtains

$$\sum_{R_{\text{mag}}} \langle\langle J_R^2 \zeta^\pm(E,\Delta E)\rangle\rangle = \sum_{R_1} J_{R_1}^2 \langle \zeta^\pm(E,\Delta E_1)\rangle_1 + \sum_{R_2} J_{R_2}^2 \langle \zeta^\pm(E,\Delta E_2)\rangle_2 = \tfrac{1}{2} N_{\text{mag}} J^2 [\langle \zeta^\pm(E,\Delta E_1)\rangle_1 + \langle \zeta^\pm(E,\Delta E_2)\rangle_2]. \quad (19)$$

We now use the fact[8] that

$$\Lambda^- = e^{-\Delta E/kT}\Lambda^+$$

and introduce (18) and (19) into (11); this yields

$$\tau(\mathbf{k}_\pm) = \hbar/(P_1^\pm + P_2^\pm), \quad (20)$$

where

$$P_1^\pm \equiv (E_F/\pi |\nabla_{\mathbf{k}} E|_{E_F})\{N_{\text{eff}} V^2 + N_{\text{mag}} \tfrac{1}{2}[\langle (V + M_s J)^2 \rangle_1 + \langle (V + M_s J)^2 \rangle_2]\}\Omega^{-1}, \quad (21)$$

$$P_2^\pm \equiv (E_F/\pi |\nabla_{\mathbf{k}} E|_{E_F})\{N_{\text{mag}} J^2 [\langle \Lambda^+ Q(\mp x,\mu_1)\rangle_1 + \langle \Lambda^+ Q(\mp x,\mu_2)\rangle_2]\}\Omega^{-1}, \quad (22)$$

$$Q(x,\mu) \equiv \frac{e^x+1}{e^{x+\mu}+1}, \quad x \equiv \frac{E-E_F}{k}, \quad \mu \equiv \frac{E}{kT}. \quad (23)$$

Slowly varying functions have been replaced by their values on the Fermi surface. We finally have

$$f_1(\mathbf{k}_\pm) = \tau^\pm e\mathcal{E}\cdot\nabla_{\mathbf{k}} f_0/\hbar. \quad (24)$$

Having determined the distribution function (24) in terms of Eqs. (20)–(23), we may now calculate the resistivity, and hence the magnetoresistance, through the standard expression[8]

$$\sigma = \frac{1}{|\mathcal{E}|}\sum_{\mathbf{k}} v_{\mathbf{k}} e[f_1(\mathbf{k}_+) + f_1(\mathbf{k}_-)] = \frac{e^2}{6\pi m}\int_0^\infty (\tau^+ + \tau^-) k^3 \frac{\partial f_0}{\partial \epsilon} d\epsilon. \quad (25)$$

The integrations may be performed analytically; the resulting combinations of elementary functions are lengthy and not transparent. We therefore do not display them. These complicated functions have been fitted to the data points mechanically by varying the parameters of the theory to minimize the squared differences between the calculated values and the data points.

V. PARAMETRIZATION

The calculation of $\Delta\rho/\rho_0$ according to our theory depends upon five parameters: (1) the total magnetic field at the impurity sites, resolved into molecular fields and externally applied field; (2) the fractional concentrations of magnetic impurities compared to nonmagnetic, $N_{\text{mag}}/N_{\text{eff}}$; (3) the ratio V/J of the parameters of magnetic and potential scattering; (4) the effective g factor or field multiplicative factor; and (5) the total-spin-angular-momentum quantum number of the impurity sites, $\mathcal{S}$. The resistivity depends as well on the absolute values of V and N; $\Delta\rho/\rho_0$ does not.

It is clear from the discussion of the preceding sections that the number of parameters cannot be reduced without seriously compromising the usefulness of the model. However, because ρ versus H is a function with few pronounced features, five parameters cannot be accurately determined by a single curve fitting. Estimates of the magnitudes of the parameters can be obtained, however, by successive fits of theory to data taken on different samples under varying conditions. Consistency of the results under such variations is a measure of the degree of reliability of the calculated parameter values.

Accordingly, we have studied on the order of a dozen samples, taken from three different crystal boules, cut along various crystallographic orientations, and measured at several temperatures. Our results were similar for every set of data; no specimen showed any qualitative departure from the over-all trend. There was wide scatter in the optimum values of each parameter, but the orders of magnitude were always consistent over the whole set.

A tabulation of results obtained by curve fitting of data from boule 133 is provided below. For reasons discussed later we have set $\mathcal{S}=\frac{5}{2}$ in the calculations; the values assigned $\mathbf{H}_{\text{mol}}$ will also be explained later.

VI. DISCUSSION

The quality of the fits was least sensitive to the value of $\mathcal{S}$, the total-spin-angular momentum quantum number of the magnetic scatterers. It is not hard to see why this should be so. For low values of the magnetic fields, the different magnetic states are nearly degenerate, and there will be substantial occupation of all states. Since ρ must be a symmetric function of H, the curve of $\rho(H)$ versus H will be accurately parabolic at low applied fields. The curvature of this parabola depends weakly on all five parameters; it is only the higher-field departures from a parabola which can yield information separating the effects of the several parameters. However, at higher fields, the relative population of the higher lying Zeeman levels is reduced, and the spins progressively come to occupy only the ground state and the first excited state. Thus the effect of the existence of higher-lying magnetic levels becomes reduced in the very range of fields where it needs study.

Slightly improved fits were consistently obtained with larger $\mathcal{S}$ values; uniformly over our data sets, $\mathcal{S}=\frac{1}{2}$ yielded the worst fits, even when the remaining four parameters were allowed to vary freely. No discernible trend existed for $\mathcal{S}\geqslant 2$. The differences in rms derivation between data fitted with the assignment $\mathcal{S}=\frac{1}{2}$ and with higher values were at most a few percent. We used $\mathcal{S}=\frac{5}{2}$ in preparing the table because we believe the magnetic scatters to be Fe^{3+} ions for which $L=0$, $\mathcal{S}=\frac{5}{2}$. Our tentative understanding of the behavior of localized d orbitals in Ti_2O_3 suggests, as we shall see, that for impurities to be active in magnetic scattering, the orbital angular momentum L must be zero, so that spin-orbit coupling is suppressed. On these grounds one should regard the V ions as being magnetically inert; we shall return to this point in detail later.

The fractional concentrations of magnetic scatterers $N_{\text{mag}}/N_{\text{eff}}$ derived from the data is approximately a few percent; the results admit of no greater precision. The V ions incorporated in the lattice in the concentration range of a few atomic percent undoubtedly are responsible for most of the scattering. A few percent of this fraction gives a magnetic scatterer concentration of the order of 100 ppm. It seems at first sight surprising that such a low concentration of magnetically active sites can account for the observed magnetoresistance effects, the more so since the saturation region had not yet been reached. The relatively large magnetic scattering cross section required to explain these findings is, however, not difficult to understand.

If only magnetic scattering occurred, i.e., if $V=0$, one should expect that the magnetoresistance should approach a theoretical limiting value of $\Delta\rho/\rho_0\rightarrow L_t=-\frac{2}{3}$. This is because the magnetic scattering which is initially proportional to S_x^2, S_y^2, and S_z^2 in low magnetic fields becomes proportional to only S_z^2 in high magnetic fields. The actual limiting values of the magnetoresistance are estimated to lie in the range $\Delta\rho/\rho_0\rightarrow L_e=-\frac{1}{4}$ to $L_e=-\frac{1}{3}$. Thus magnetic scattering in our samples has been diluted to the extent that the limiting $\Delta\rho/\rho_0$ values have changed from L_t to L_e. Therefore, $\frac{3}{2}$ of L_e should represent the fractional contribution of the magnetic scattering process to the observed value of ρ_0 in our samples; we conclude that only from 33–50% of the ρ_0 can be attributed to magnetic scattering processes. This should be contrasted with the fact that, according to Table II, the fraction of magnetically active sites to total impurity scatterers, $N_{\text{mag}}/N_{\text{eff}}$, is in the range

TABLE II. Tabulation of parametric fits for boule 133. $\mathcal{S}=\frac{5}{2}$.

Orient.	T (°K)	g	T_c (°K)	N_{mag}/N_{eff}	$\lvert V/J\rvert$	H_{mol} (kG)
45° c	4.2	0.50	−4.2	0.032	0.64	−0.004
$\perp a$	4.2	0.58	−3.0	0.010	0.36	−0.002
$\perp a$	2.0	0.39	−3.2	0.046	0.85	−1.41
$\perp c$	2.0	0.46	−2.0	0.026	0.56	0.000
$\parallel c$	2.0	0.34	−3.9	0.042	0.77	0.000

1–5%. Typically, the magnetic cross section, must exceed the nonmagnetic by a factor of 20.

We can, in a simple approximation, take the efficacy of scattering by neutral and by magnetic centers as proportional to V^2 and to $J^2\mathcal{S}^2$, respectively. Using the values of $\mathcal{S}=\frac{5}{2}$ and $V/J=0.5$ as given in Table II, we see that $J^2\mathcal{S}^2$ exceeds V^2 by a factor of 25. Since neither the condition $J\approx 2V$ nor the value $\mathcal{S}=\frac{5}{2}$ is unreasonable, the strong influence of the greatly outnumbered magnetic scattering centers is accounted for by the model.

We consider now the state of the V ions in the oxide. Experimentally, it is found that V-doped Ti_2O_3 is p-type material and that the V ions do not appear to contribute to magnetic scattering. This can be explained through several possible models. First, both facts may be rationalized on the basis that a fraction or all of the vanadium is incorporated in the host as V^{2+} ion. This is not an unreasonable assertion, since thermodynamic data[9] indicate that the free energies of formation of VO and V_2O_3 are nearly identical under the conditions of crystal growth. If our tentative assertion is correct, one concludes that every V^{2+} ion introduces a hole into the d-like bands of primarily cationic character through charge compensation, i.e., by the concomitant creation of Ti^{4+} ions. In these circumstances, the d-like A_{1g} bands which are normally filled[10] lose one electron per Ti^{4+} ion.

It has been recognized for some time[11] that the d bands in V oxides are much narrower than those in Ti oxides, indicating a substantially tighter binding of d electrons to V ions than to Ti ions. In a Ti_2O_3 host lattice where there is only one d electron per Ti ion, both the greater nuclear charge of the V ion and the possibility of an intra-atomic exchange interaction between the multiple d electrons of the V ion will contribute to the relatively tighter binding of electrons to V. Localized d levels of the V ion should lie well below the corresponding d bands of the host lattice. Thus, not only the V^{3+} levels, but even the higher lying V^{2+} levels may lie below the top of the filled A_{1g} bands of the host. In this case, even with perfect stoichiometry, V doping will produce holes in the filled Ti_2O_3 bands.

As a second possibility, deviations from stoichiometry may also increase the hole concentration. Under the conditions of growth of our crystals, a significant cation deficiency may occur as a side effect (actually, V free crystals showed such an effect).[1] In this event three holes would be introduced into the d-like A_{1g} band for every cation deficiency. Unfortunately, present-day analytical techniques are not adequate for the delicate task of checking small deviations from perfect stoichiometry. In any case, either mechanism for introducing holes offers a reasonable explanation of the experimental fact that our doped crystals were observed to be p type.

We now show that the V^{2+} or the V^{3+} ion can very well be magnetically inactive. This may be understood through the discussion of Ref. 12. There it is shown that under the combined effects of a cubic field with a trigonal component (as prevails at cationic sites of the corundum structure), spin-orbit coupling, and of a magnetic field, the ${}^4A_{2g}$ state of V^{2+} is split into two Kramers doublets characterized by $\mathcal{S}_z=\pm\frac{3}{2}$ and $\mathcal{S}_z=\pm\frac{1}{2}$. Similarly, the ${}^3T_{1g}$ state of V^{3+} is split into a nondegenerate $\mathcal{S}_z=0$ level, and a doublet for which $\mathcal{S}_z=\pm 1$. The V^{3+}, $\mathcal{S}_z=0$ state is obviously magnetically inert. The V^{2+}, $\mathcal{S}_z=\pm\frac{3}{2}$ and V^{3+}, $\mathcal{S}_z=\pm 1$ doublet states consist of two levels whose associated spin angular momenta differ by $3\hbar$ and $2\hbar$, respectively. Hence transitions between these sublevels induced by spin flip scattering or by photon absorption are forbidden; these atomic states are thus also magnetically inert. However, transitions are allowed between the sublevels of the V^{2+}, $\mathcal{S}_z=\pm\frac{1}{2}$ doublet. To rationalize the fact that V scattering centers are neutral, one must thus postulate (a) that the V^{2+}, $\mathcal{S}_z=\pm\frac{3}{2}$ state lies lower in energy than the $\mathcal{S}_z=\pm\frac{1}{2}$ state, (b) that the latter is thermally inaccessible under the conditions of our experiment, and (c) that the atomic V^{3+}, $\mathcal{S}_z=0$ and $\mathcal{S}_z=\pm 1$ are also split by an energy difference largely relative to kT, so that transitions between the $\mathcal{S}_z=0$ and $\mathcal{S}_z=+1$ or $\mathcal{S}_z=-1$ levels are frozen out. These assumptions are well in accord with typical spin-orbit interaction energies encountered in this region of the periodic table.

In the case of an Fe^{3+} ion that enters the Ti_2O_3 lattice. the five d electrons combine to produce an orbital singlet, with $L=0$. In these circumstances, the $\mathcal{S}=\frac{5}{2}$ sextet levels are not split by spin-orbit coupling, and the ion will be magnetically active. Our samples had iron concentrations of the order of a 100 at. ppm, which is consistent with the experimental findings that only 1–5% of the 2–4% impurities present in doped Ti_2O_3 were magnetically active.

Our idea of the role of V in the Ti_2O_3 lattice is not uniquely forced by the data; more, as well as different, experiments would be needed to obtain a completely convincing picture. Nonetheless, the experimental facts are that the V doped material is p type and that V ions are magnetically inert. These facts, which seem surprising on a first, cursory inspection, are seen to be

[9] C. E. Wicks and F. E. Block, U. S. Bureau of Mines Bulletin 605 (1963).
[10] W. Kleiner, MIT Lincoln Laboratory Solid State Research Report No. 3, 1967, p. 44 (unpublished).
[11] D. Adler, Solid State Phys. 21, 1 (1968).
[12] C. J. Ballhausen, *Introduction to Ligand Field Theory* (McGraw-Hill Book Co., New York, 1962), pp. 230–235.

parts of a reasonable and consistent model, which thus need not be labeled as "strange." [13]

From Table II it is evident that V/J has a value of roughly 0.5, so that there is an approximate equity in the nonmagnetic and magnetic scattering potentials. There were actually two optimum fits, corresponding to $+|V/J|$ and $-|V/J|$. The properties of the scattering are slightly different for these two because of the difference in interference between the two types of scattering on the same site, $(|V|+m_sM_s|J|)^2$ and $(|V|-m_sM_s|J|)^2$. The differences are too small to be meaningful, and we can draw no conclusions about the relative signs of V and J.

The effective field-multiplicative constant has values in the range 0.4–0.6. The argument of the functions of our theory is the ratio of Zeeman splitting to temperature, $g\mu H/kT$. This suggests that there is no unique way of assigning the multiplicative constant, either to g, H, or T. Sasaki,[13] considering a similar system, has interpreted his results in terms of a Curie temperature subtracted from the actual temperature T,

$$T_{\text{eff}}=T-T_C.$$

He chooses this phenomenology in analogy with the Curie temperature which appears in the theory of magnetic susceptibility. Following his method we have therefore listed, in Table II, T_C values as determined from our data. The significance of these values is difficult to assess, because the actual g factor of the ions may be less than 2.

The most interesting parameter of our theory is the magnetic field at the scattering sites, composed of the externally applied field and the molecular field. If this oxide were antiferromagnetic, one would expect to encounter molecular fields typically of the order of hundreds of kilogauss, or, because of the small moments reported on the Ti, to encounter fields no less than several tens of kilogauss. Since the axis of orientation of the potential molecular field, if any, was unknown but was expected to lie along or near a crystal symmetry direction, we oriented the external fields in directions of high crystal symmetry. We should then have encountered the special cases where $\mathbf{H}_{\text{ext}}$ is either perpendicular to or parallel with $\mathbf{H}_{\text{mol}}$. The former would give rise to a single value for the magnitude of the field on all sites, $\mathbf{H}_{\text{tot}}=(H_{\text{ext}}^2+H_{\text{mol}}^2)^{1/2}$ and the latter values would give rise to the values $\mathbf{H}_{\text{tot}}^{(1)}=\mathbf{H}_{\text{ext}}+\mathbf{H}_{\text{mol}}$, and $\mathbf{H}_{\text{tot}}^{(2)}=\mathbf{H}_{\text{ext}}-\mathbf{H}_{\text{mol}}$. We therefore analyzed our data trying both these possibilities. The results were the same in both cases, namely, that $\mathbf{H}_{\text{mol}}=0$. The table gives values for the optimal $\mathbf{H}_{\text{mol}}$ obtained from curve fitting with the assumption $\mathbf{H}_{\text{tot}}=(H_{\text{ext}}^2+H_{\text{mol}}^2)^{1/2}$.

Our curve-fitting procedure required an initial guess at the parameters, and for $\mathbf{H}_{\text{mol}}$ we used 100 kG. One run of data gave a local minimum in the mean-squared deviation at 96 kG, in addition to one at zero, but this minimum required J to exceed V by a factor of 10^4, and we ruled out this single case.

The precise vanishing of the molecular field appears as a result of our curve fitting, but qualitatively we can see that any molecular fields must be anomalously small if our model is even approximately applicable. A large internal field would be inconsistent with the substantial magnetoresistance we observed unless either the V ions were magnetically active or V/J were radically different from what we found it to be (as in our single case above). The possibility of the V ions acting as magnetic scatterer in our samples has been examined by Weber[14] in rf magnetic resonance experiments. He obtained resonance peaks consistent with our low concentration magnetic scatters, but inconsistent with what is anticipated if V were magnetically active. A much more extensive series of such experiments would, however, be necessary to rule out this possibility completely.

While we have not constructed an overwhelming case against the existence of antiferromagnetism in Ti_2O_3 or, at least in V-doped Ti_2O_3 containing minor impurities, there is an over-all consistency in our model which strongly supports the hypothesis that no long-range magnetic order exists in Ti_2O_3. This finding is buttressed by other experimental evidence that has been recently summarized by Honig.[2]

ACKNOWLEDGMENTS

The authors are pleased to acknowledge the generous assistance they received from staff members of the Francis Bitter National Magnet Laboratory, in carrying out the measurements at high magnetic fields. They are also indebted to Dr. J. B. Goodenough and Dr. W. H. Kleiner of the MIT Lincoln Laboratory for stimulating discussions concerning the interpretation of the results.

[13] W. Sasaki, J. Phys. Soc. Japan **20**, 825 (1965).

[14] R. Weber (private communication).